MATHEMATICAL BIOSCIENCES
AND ENGINEERING
Volume **12**, Number **6**, December **2015**

doi:10.3934/mbe.2015.12.1157

pp. **1157–1172**

A DATA-MOTIVATED DENSITY-DEPENDENT DIFFUSION MODEL OF IN VITRO GLIOBLASTOMA GROWTH

Tracy L. Stepien, Erica M. Rutter and Yang Kuang

School of Mathematical & Statistical Sciences
Arizona State University
Tempe, AZ 85287-1804, USA

Abstract. Glioblastoma multiforme is an aggressive brain cancer that is extremely fatal. It is characterized by both proliferation and large amounts of migration, which contributes to the difficulty of treatment. Previous models of this type of cancer growth often include two separate equations to model proliferation or migration. We propose a single equation which uses density-dependent diffusion to capture the behavior of both proliferation and migration. We analyze the model to determine the existence of traveling wave solutions. To prove the viability of the density-dependent diffusion function chosen, we compare our model with well-known in vitro experimental data.

1. **Introduction.** Glioblastoma multiforme is a malignant form of brain cancer with an especially grim prognosis—mean survival time from detection is less than 15 months (Norden and Wen [20]). Glioblastoma are characterized not only by intense proliferation, but also by excessive migration. This leads to an inability to effectively treat the tumors, as surgical resection is able to remove the core of the tumor, but not the migratory cells. This erratic behavior makes modeling all aspects of glioblastoma growth difficult.

Early models of glioblastoma growth include reaction-diffusion equations which are able to accurately capture the proliferating tumor core. Tracqui et al. [30] formulated the earliest reaction-diffusion model to describe glioblastoma growth and diffusion, also with therapeutic intervention. Swanson et al. [29] continued with these reaction-diffusion models, accounting for a spatially dependent diffusion model in an attempt to model more heavily the migratory behavior of the tumor cells.

A landmark mathematical model introduced by Stein et al. [27] advocated for the separation of glioblastoma cells into two separate populations: the proliferating core cells and the migratory cells. Their model was based off of observations from in vitro experiments involving the spreading of two human astrocytoma cell lines that form tumor spheroids. In addition to the standard reaction-diffusion terms in the equation for migratory cells, the Stein et al. [27] model includes a radially biased motility term corresponding to convection to account for the situation where cells detect the location of the tumor core and actively move away from it. Our goal is to formulate a single equation which captures both the migratory and core tumor

2010 *Mathematics Subject Classification.* Primary: 92C50, 35C07; Secondary: 35K57.

Key words and phrases. Biomathematical modeling, glioblastoma, traveling waves, tumor growth simulation.

characteristics as accurately as the dual-equation approach, by using a density-dependent diffusion term.

One of the fundamental questions with in vitro tumor growth is how fast is the tumor growing? Can we estimate how far the tumor will spread after a certain amount of time? We want to quantify tumor spread, not just computationally, but also analytically. To this end, we will need to analyze the traveling wave solutions.

Traveling wave solutions have been studied in models of glioblastoma growth with multiple cell populations and constant diffusion, such as in Pérez-García et al. [23] and Harko and Mak [8]. Traveling wave solutions also arise in density-dependent reaction-diffusion equations, and numerous density-dependent diffusion functions have been studied by, for example, Atkinson et al. [2], Murray [18], Witelski [31], Sánchez-Garduño and Maini [24], Harris [9], Pedersen [22], Maini et al. [13], Sánchez-Garduño et al. [25], Ngamsaad and Khompurngson [19], and Kengne et al. [11]. More generally, traveling wave solutions for convective-reaction-diffusion equations were studied in Malaguti et al. [14, 15, 16] and Gilding and Kersner [7]. Minimal speeds for various diffusion and convective terms were estimated.

In this article, we study a nondegenerate convective-reaction-diffusion equation model of glioblastoma tumor growth. The existence of traveling waves is analyzed and the minimum wave speed is corroborated by simulations. We perform a sensitivity analysis on the parameters in the model to detect how variations in parameters effect the numerical solution. Lastly, we optimize the parameters in order to validate the model with in vitro experimental data. We show that this single equation model fits the data as well as the previously posed two-equation model of Stein et al. [27].

2. **Model formulation.**

Multiple mathematical models have attempted to explain and predict the proliferation and migration of the glioblastoma tumor cells in vitro and in vivo with varying success (see the review paper by Martirosyan et al. [17] and references therein). The growth and diffusion of malignant glioma are governed by many processes including, but not limited to, random diffusion, chemotaxis, haptotaxis, cell-cell adhesion, cell-cell signaling, and microenvironmental cues such as oxygen and glucose. Our proposed model is a variation on the in vitro mathematical model of Stein et al. [27]. We briefly discuss the original experiment and mathematical model and then the reasoning behind our alterations.

In Stein et al. [27], two human astrocytoma U87 cell lines are implanted into gels—one with a wild-type receptor (EGFRwt) and one with an over expression of the epidermal growth factor receptor gene (ΔEGFR). The resulting spheroids were left to grow over 7 days and imaged every day. We show a summary of the results of the experiment for the invasive and proliferating cell radii on days 0, 1, 3, and 7 in Figure 1. The tumor core radius was measured to be where pixels had an intensity of < 0.12 and the invasive radius as the half-maximum for the image averaged over the azimuthal angle.

The mathematical model proposed by Stein et al. [27] describes the movement of the invasive, or migratory, cells (u_i) for the EGFRwt cell line and the ΔEGFR cell line based on the experiment described above. The radius of the tumor core, consisting of the less mobile cells, is modeled as increasing at a constant rate based on the in vitro experimental data. The model of Stein et al. [27] assumes that the tumor cells leave the tumor core and become invasive cells to invade the collagen gel. The behavior of invasive cells is described by the model in a way that can

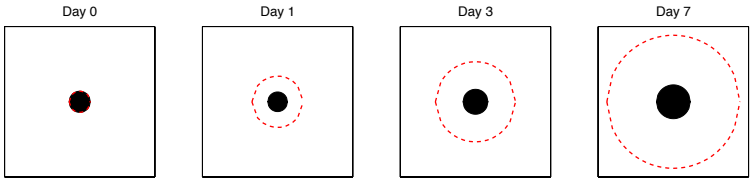

FIGURE 1. The radius of the core proliferating (black) and migratory (red dashed) cells for the experiment for EGFRwt strain from Stein et al. [27] on days 0, 1, 3, and 7. The domain is a 3 mm by 3 mm square.

be quantitatively compared to the experimental measurements. The invasive cell population is governed by the following ad hoc partial differential equation

$$\frac{\partial u_i(r,t)}{\partial t} = \underbrace{D\nabla^2 u_i}_{\text{diffusion}} + \underbrace{g u_i\left(1-\frac{u_i}{u_{\max}}\right)}_{\text{logistic growth}} - \underbrace{\nu_i \nabla_r \cdot u_i}_{\text{taxis}} + \underbrace{s\delta(r-R(t))}_{\text{shed cells from core}}, \tag{1}$$

where u_i represents the invasive cells of the tumor at radius r and time t (Stein et al. [27]). The forces acting upon the invasive cell population are random diffusion, logistical growth, taxis, and cells being shed from the core of the tumor. Taxis refers to the active biased motility of invasive cells away from the tumor core which Stein et al. [27] attributes to possibly chemotaxis or haptotaxis. This taxis term was found to be more necessary for the highly invasive EGFRwt strain compared to the less invasive ΔEGFR strain.

As the core of the tumor increases, cells are shed from the front of the expanding core to become invasive cells. Parameter D is the diffusion constant, g is the growth rate, $u_{\max}$ is the carrying capacity, ν_i is the degree at which cells migrate away from the core, s is the amount of cells shed per day, and δ is the Dirac delta function. The radius of the tumor core is modeled by $R(t) = R_0 + \nu_c t$, where R_0 is the initial radius of the tumor core and ν_c is the constant velocity at which the tumor core radius increases.

The experimental data in Stein et al. [27] suggests that the invasive cell radius also spreads at a constant velocity. However, the assumption that the tumor core radius increases at a constant rate and the existence of the Dirac delta function in equation (1) is rather artificial and makes traveling wave analysis of the invasive cells very difficult. We therefore extend the model of Stein et al. [27] to alleviate some of these issues.

We build our model from a similar base. We keep the logistic growth term, as we know that the tumor cells grow in number, and logistic growth is sensible. We also keep the taxis term, since it is apparent that glioblastoma tumor cells do migrate away from the tumor core (Stein et al. [28]). Since we are trying to model the tumor core in addition to the invasive cells, we do not need to consider the cell shedding term. Although many current cancer cell migration models are based on reaction-diffusion equations, most of those models consider diffusion to be constant or as a function of space. Some cell migration models have included density-dependent diffusion, such as the wound healing model of Cai et al. [4].

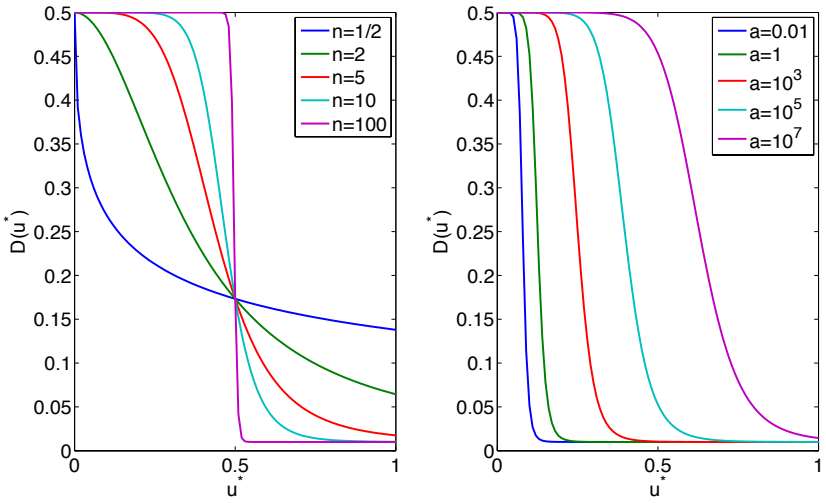

FIGURE 2. The density-dependent diffusion function $D(u^*)$, where $u^* = \frac{u}{u_{\max}}$, from Equation (3) for $D_1 = 0.5$, $D_2 = 0.4$, and various a and n. As u^* increases, $D(u^*)$ decreases from its maximum D_1 to its minimum $D_1 - D_2$.

We consider a density-dependent convective-reaction-diffusion equation, which implies that the amount of random diffusion depends on how many cells are present. Our governing equation for the tumor cells $u(x,t)$ is thus

$$\frac{\partial u}{\partial t} = \underbrace{\nabla \cdot \left(D\left(\frac{u}{u_{\max}}\right) \nabla u \right)}_{\text{density-dependent diffusion}} + \underbrace{gu\left(1 - \frac{u}{u_{\max}}\right)}_{\text{logistic growth}} - \underbrace{\operatorname{sgn}(x)\nu_i \nabla \cdot u}_{\text{taxis}}, \tag{2}$$

where we consider the equation in Cartesian coordinates but assume there is radial symmetry. Parameters g and ν_i are as in equation (1), but now they are in relation to the entire tumor cell population instead of just the invasive cell population.

There are many functions that could serve as the density-dependent diffusion $D(u^*)$, where $u^* = \frac{u}{u_{\max}}$. Experimental work from Stein et al. [27] suggests that diffusion is large for areas where the cell density is small (the migrating tumor cells), but diffusion is small where the cell density is large (the proliferating tumor cells). This relation could possibly be explained by cell–cell adhesion (Armstrong et al. [1]). To capture this behavior, we set

$$D(u^*) = D_1 - \frac{D_2 (u^*)^n}{a^n + (u^*)^n}. \tag{3}$$

For biologically relevant parameters, we assume that D_1, D_2, g, a, and ν_i are all positive, $n > 1$, and $D_2 \leq D_1$ to avoid "negative" diffusion, which is a problem both biologically and numerically. See Figure 2 for an illustration of the density-dependent diffusion function (3) for various a and n. The parameter n governs how steeply the function decreases and the parameter a governs the u^* value at which the transition is occurring at half maximal rate. D_1 and D_2 govern the range of the function.

As we consider the biology of tumor growth, we recall that glioblastoma tumor cells must be considered as two differing populations. The proliferative cells are assumed to remain somewhat stationary and diffuse slowly but grow in population quickly. On the other hand, the migrating cells diffuse very quickly, traveling very far in a short amount of time, but do not grow in population as quickly. Since the proliferating cells are the tumor core cells, they occur when cell density is very high, and the migrating cells are where the cell density is very low. For our application, we choose $D_2 \leq D_1$, which allows diffusion to be small for proliferating cells and larger for migrating cells.

3. **Traveling wave speed analysis.** In this section we analyze the existence of traveling wave solutions of (2) using phase plane analysis.

Rewriting (2) in one-dimensional Cartesian coordinates, the governing equation is

$$\frac{\partial u}{\partial t} = D\left(\frac{u}{u_{\max}}\right)\frac{\partial^2 u}{\partial x^2} + \frac{1}{u_{\max}}D'\left(\frac{u}{u_{\max}}\right)\left(\frac{\partial u}{\partial x}\right)^2 - \nu_i\frac{\partial u}{\partial x} + gu\left(1 - \frac{u}{u_{\max}}\right). \quad (4)$$

Rescale by writing

$$t^* = gt, \qquad x^* = x\sqrt{g}, \qquad u^* = \frac{u}{u_{\max}}, \quad (5)$$

set

$$v = \frac{\nu_i}{\sqrt{g}}, \quad (6)$$

and, omitting the asterisks and dividing through by $gu_{\max}$ for simplicity, the equation (4) becomes

$$\frac{\partial u}{\partial t} = D(u)\frac{\partial^2 u}{\partial x^2} + D'(u)\left(\frac{\partial u}{\partial x}\right)^2 - v\frac{\partial u}{\partial x} + u\,(1-u)\,. \quad (7)$$

A traveling wave solution of (7) is a solution of the form

$$u(x,t) = w(x - kt), \quad (8)$$

where $k \geq 0$ is the speed of the traveling wave and the function $w(z)$ is defined on the interval $(-\infty, \infty)$ and satisfies the boundary conditions

$$\lim_{z\to-\infty} w(z) = 1, \qquad \lim_{z\to\infty} w(z) = 0. \quad (9)$$

Substituting ansatz (8) into (7) results in the second-order ordinary differential equation

$$w''(z) + \frac{1}{D(w(z))}\Big((k-v)w'(z) + D'(w(z))(w'(z))^2 + w(z)(1-w(z))\Big) = 0, \quad (10)$$

which we may write in this form because the function D as in equation (3) is always positive.

Rewriting (10) as a system of first-order ordinary differential equations by setting $y := dw/dz$,

$$w' = y, \quad (11a)$$

$$y' = \frac{-1}{D(w)}\Big((k-v)y + D'(w)y^2 + w(1-w)\Big). \quad (11b)$$

This system has two equilibrium points, $(w, y) = (0, 0)$ and $(w, y) = (1, 0)$.

The Jacobian matrix evaluated at $(1,0)$ is

$$J(1,0) = \begin{pmatrix} 0 & 1 \\ \frac{1}{D(1)} & \frac{-(k-v)}{D(1)} \end{pmatrix}, \tag{12}$$

from which we have $\det J(1,0) = \frac{-1}{D(1)} < 0$, and thus $(1,0)$ is a saddle equilibrium point.

The Jacobian matrix evaluated at $(0,0)$ is

$$J(0,0) = \begin{pmatrix} 0 & 1 \\ \frac{-1}{D(0)} & \frac{-(k-v)}{D(0)} \end{pmatrix}, \tag{13}$$

from which we have $\det J(0,0) = \frac{1}{D(0)} > 0$ and assuming that $k > v$, then $\operatorname{tr} J(0,0) = \frac{-(k-v)}{D(0)} < 0$ and $(0,0)$ is a stable node or spiral. Since a stable spiral cannot result in physiologically relevant solutions, we obtain the condition

$$k \geq k_{\min} = 2\sqrt{D_1} + v, \tag{14}$$

which in terms of the original dimensional equation (4) is

$$k \geq k_{\min} = 2\sqrt{D_1 g} + \nu_i. \tag{15}$$

We will prove the following main result.

Theorem 3.1. *There exists a traveling wave solution (8) of the partial differential equation (7) with boundary conditions $u(x,t) \to 1$ as $x \to -\infty$ and $u(x,t) \to 0$ as $x \to \infty$ with $0 < u(x,t) < 1$, whose orbit connects the steady states $u \equiv 0$ and $u \equiv 1$ if and only if (14) is satisfied.*

To do so, we need to construct a positively invariant region in which to trap the unstable manifold of the saddle point. Figure 3 illustrates a positively invariant trapping region and the heteroclinic orbit connecting the two equilibrium points for a set of physiologically relevant parameters.

Since the horizontal ($w' = 0$) nullcline is the horizontal axis $\{y = 0\}$, the flow across this line (when $w \in (0,1)$) is perpendicular in the negative y direction. Define the line

$$\mathcal{T}_1 = \{(w,y) : 0 \leq w \leq 1,\ y = 0\}. \tag{16}$$

Next, consider the line that corresponds to the eigenvector corresponding to the more negative eigenvalue of the linearized system at $(0,0)$, i.e.,

$$y(w) = \alpha_0 w, \tag{17}$$

where we define

$$\alpha_0 = \frac{1}{2D(0)}\left(-(k-v) - \sqrt{(k-v)^2 - 4D(0)}\right). \tag{18}$$

Note that $\alpha_0 < 0$.

Lemma 3.2. *The flow at any point along the line $y(w) = \alpha_0 w$, for $w \in (0,1]$, crosses that line in the positive y direction for k sufficiently small.*

Proof. The normal vector to the graph of $(w, \alpha_0 w)$ pointing in the positive y direction is $(-\alpha_0, 1)$. Restricting the vector field to points along the line $y(w) = \alpha_0 w$

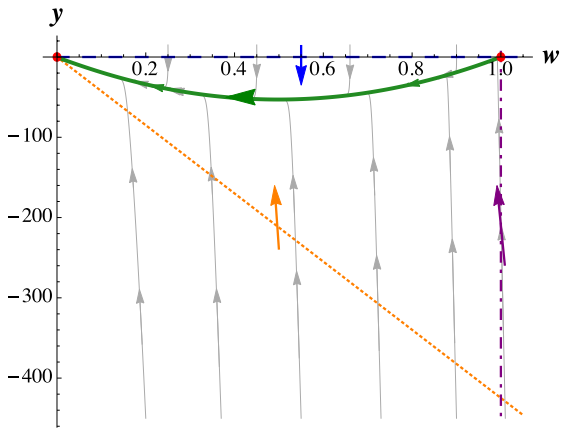

FIGURE 3. Phase Portrait of the system (11) with parameter values (37). The solid green curve is the unstable manifold, the dashed blue curve is $\mathcal{T}_1$ (16) the vertical nullcline, the dotted orange line is $\mathcal{T}_2$ (28) corresponding to the eigenvector of linearized system at $(0,0)$, and the dash-dotted purple line is $\mathcal{T}_3$ (30). Arrows show direction of flow. The nondimensional wave speed $k = 2\sqrt{D_1} + v = 2\sqrt{D_1} + \nu_i/\sqrt{g} \approx 0.0047746$.

results in the system

$$w' = \alpha_0 w, \tag{19a}$$

$$y' = \frac{-1}{D(w)}\Big((k-v)\alpha_0 w + D'(w)\alpha_0^2 w^2 + w(1-w)\Big). \tag{19b}$$

We choose k such that the inner product $(-\alpha_0, 1)\cdot(w', y') \geq 0$ along the graph of $(w, \alpha_0 w)$, and thus

$$-\alpha_0^2 w - \frac{1}{D(w)}\Big((k-v)\alpha_0 w + D'(w)\alpha_0^2 w^2 + w(1-w)\Big) \geq 0, \tag{20}$$

which can be rearranged as

$$-\frac{\alpha_0 w}{D(w)}\left(\alpha_0 D(w) + (k-v) + D'(w)\alpha_0 w + \frac{1-w}{\alpha_0}\right) \geq 0. \tag{21}$$

Since $\alpha_0 < 0$ and $D(w) > 0$ for $w \in (0,1]$, then $-\frac{\alpha_0 w}{D(w)} > 0$ and the inequality becomes

$$\alpha_0 D(w) + (k-v) + D'(w)\alpha_0 w + \frac{1-w}{\alpha_0} \geq 0. \tag{22}$$

Since (22) must hold for all $w \in [0,1]$, then we obtain the condition

$$k \geq v - \max_{w\in[0,1]}\left\{\frac{d}{dw}\big(D(w)(\alpha_0 w)\big) - \frac{w(1-w)}{\alpha_0 w}\right\}. \tag{23}$$

However, since α_0 depends on k, substitute (18) into (23), and after tedious algebraic manipulation the inequality becomes

$$k \leq v + \min_{w\in[0,1]}\left\{\frac{D(w) + wD'(w) - D_1(1-w)}{\sqrt{w(D(w) + wD'(w) - D_1)}}\right\}. \tag{24}$$

Consider the function

$$h(w) = \frac{D(w) + wD'(w) - D_1(1-w)}{\sqrt{w(D(w) + wD'(w) - D_1)}}. \tag{25}$$

The minimum of $h(w)$ is attained in the interior of the domain $[0,1]$ if $h'(w) = 0$ for some $w \in (0,1)$. This means that either (i) $D_1(1+w) - \frac{d}{dw}(wD(w)) = 0$ or (ii) $D_1 - D(w) + w\frac{d}{dw}(wD'(w)) = 0$. In case (i), this means that the diffusion function must be of the form $D(w) = D_1(1+w) + \frac{C_1}{w}$, where C_1 is an arbitrary constant. In case (ii), the diffusion function must be of the form $D(w) = D_1 + C_1\frac{w^2-1}{w} + iC_2\frac{w^2-1}{2}$, where C_1 and C_2 are arbitrary constants. Since our diffusion function (3) is of neither of these forms, the minimum cannot be attained in the interior of $[0,1]$ and must be attained at either of the endpoints $w = 0$ or $w = 1$.

Since $h(w)$ tends to infinity as $w \to 0$ (assuming that parameter $n > 1$), then the minimum occurs at $w = 1$, and thus if the condition

$$k \le v + \frac{D(1) + D'(1)}{\sqrt{D(1) + D'(1) - D_1}} = v + \frac{(a+1)^2 D_1 + (1+a+an)D_2}{(a+1)\sqrt{(1+a+an)D_2}} \tag{26}$$

is satisfied, then the lemma holds. □

Since

$$2\sqrt{D_1} \le \frac{(a+1)^2 D_1 + (1+a+an)D_2}{(a+1)\sqrt{(1+a+an)D_2}}, \tag{27}$$

the flow across the line

$$\mathcal{T}_2 = \{(w,y) : 0 \le w \le 1,\ y = \alpha_0 w\} \tag{28}$$

is in the positive y direction for at least the minimum wave speed k. For larger speeds, the nonlinearities of the system require that $\mathcal{T}_2$ be nonlinear such that

$$k \le v - \max_{w\in[0,1]} \left\{ \frac{d}{dw}\big(D(w)f(w)\big) - \frac{w(1-w)}{f(w)} \right\}, \tag{29}$$

is satisfied for some function f where $f(0) = 0$ and $f(w) \le 0$ for $w \in (0,1]$. The minimum wave speed is determined by taking the infimum on the set of functions f (Sánchez-Garduño et al. [25]).

Also due to the nonlinearities of the system and the behavior of the system near $(1,0)$, it is difficult to use the eigenvector of the linearized system at $(1,0)$ as a portion of the boundary of the trapping region, as is standard for the Fisher–Kolmogorov equation (Chicone [5]). Instead, define

$$\mathcal{T}_3 = \{(w,y) : w = 1,\ \alpha_0 \le y \le 0\}. \tag{30}$$

The flow across this line is in the negative w direction. Thus, if we define the triangle $\mathcal{T}$ defined by the boundaries $\mathcal{T}_1$, $\mathcal{T}_2$, and $\mathcal{T}_3$, then $\mathcal{T}$ is a positively invariant set.

We now prove our main result.

Proof of Theorem 3.1. We first show that the unstable manifold of the saddle point $(w,y) = (1,0)$ has nonempty intersection with $\mathcal{T}$ for all time.

The vertical ($y' = 0$) nullclines are the solutions to the quadratic equation

$$D'(w)y^2 + (k-v)y + w(1-w) = 0, \tag{31}$$

which are

$$y_+(w) = \frac{1}{2D'(w)}\Big(-(k-v) + \sqrt{(k-v)^2 - 4D'(w)w(1-w)}\Big), \tag{32a}$$

$$y_-(w) = \frac{1}{2D'(w)}\Big(-(k-v) - \sqrt{(k-v)^2 - 4D'(w)w(1-w)}\Big). \tag{32b}$$

Since $k > v$, the slope of the y_+ nullcline at $w = 1$ is

$$y'_+(1) = \frac{1}{k-v} > 0, \tag{33}$$

and the eigenvector of the linearized system corresponding to the positive eigenvalue at the saddle point $(1, 0)$ is

$$\vec{\eta} = \left(1, \quad \frac{1}{2}\left(\frac{-(k-v)}{D(1)} + \sqrt{\left(\frac{k-v}{D(1)}\right)^2 + \frac{4}{D(1)}}\right)\right)^T. \tag{34}$$

All trajectories that leave the point $(1, 0)$ in the region $\mathcal{R} = \{(w, y) : 0 \le w \le 1,\ y \le 0\}$ have the tangent vector $\vec{\eta}$ at $(1, 0)$. Comparing the slope of eigenvector $\vec{\eta}$ and the slope of the y_+ nullcline at the point $(1, 0)$, we find that the slope of $\vec{\eta}$ is less than the slope of y_+. Therefore, trajectories leaving point $(1, 0)$ leave above y_+. Since the flow across the nullcline y_+ is perpendicular in the negative w direction, and y_+ is contained in $\mathcal{T}$ near $w = 1$, the unstable manifold of the saddle at $(1, 0)$ has nonempty intersection with $\mathcal{T}$.

Thus, the unstable manifold of the saddle at $(1, 0)$ remains in the region $\mathcal{T}$ for all time, and furthermore, the ω-limit set of the corresponding orbit is also in $\mathcal{T}$. Since $w' = y \le 0$ within $\mathcal{T}$, by the Poincaré–Bendixson theorem, there are no periodic orbits or equilibrium points in the interior of $\mathcal{T}$. The ω-limit set must be contained in the boundary of $\mathcal{T}$, and therefore, the ω-limit set is $(0, 0)$.

Hence, there exists a heteroclinic orbit connecting the equilibrium points $(w, y) = (0, 0)$ and $(w, y) = (1, 0)$ as long as the condition (14) is satisfied, which implies that a traveling wave solution exists. □

Thus, we should expect in our numerical simulations that the wave speed of the invasive cells is constant and satisfies condition (15).

4. **Computational results.** In order to show that the proposed model is viable, we compare numerical simulations with experimental data and the traveling wave analysis. A sensitivity analysis as well as a parameter optimization to fit the experimental data is performed. Finally, the simulated wave speed is compared with the minimum wave speed (15) derived in the previous section.

Experimental data provided in Stein et al. [27] includes the density profile of cells on day 3 and the invasive radius of the cells measured from days 1 through 7 for both the U87WT and U87ΔEGFR cell lines. The data was obtained via GRABIT [6], a MATLAB program which extracts data points from an image file. We concentrate on the U87WT cell line because we want to show our model is effective even for the strongest migratory cells. All simulations are performed with the U87WT cell line in mind and are compared to the U87WT data.

The numerical simulations are run over a large spatial domain and boundary conditions specify that there are no tumor cells at the boundaries, in other words, $u(x, t) = 0$ when $x = \pm 1$ cm. This ensures that the tumor can freely move within the domain. Stein et al. [27] does not model the tumor core cells in the invasive cell

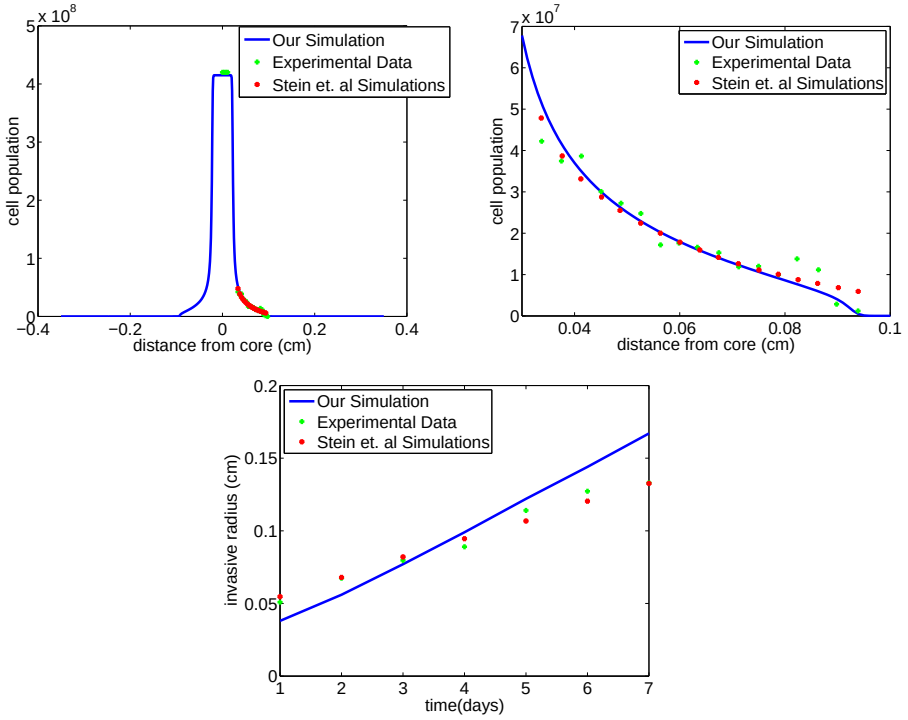

FIGURE 4. Numerical solution of the density-dependent diffusion glioblastoma model (2) with diffusion function (3) and optimized parameter values (37) compared to experimental data from Stein et al. [27] and their simulations. The density profile is from day 3 of the experimental data.

equation (1), and the initial cell density for their simulations was zero. However, our model (2) contains all tumor cells. From Stein et al. [27], the initial core tumor radius is 210μm and the maximum cell density is $u_{\max} = 4.2 \times 10^8$ cells/cm^3, and thus we assume that initially the cell density is 95% of $u_{\max}$ for the initial core tumor radius of 210μm and zero elsewhere.

The governing equation (2) is discretized using the Crank-Nicolson method for the density-dependent diffusion term and first-order forward differencing for the advection and logistic growth terms. For the advection term on the left hand side, first-order backward differencing is used. A limited spatio-temporal study was conducted to determine the largest possible spatial step and time steps which would still produce accurate results. Our method was compared with results from the MATLAB program pdepe [26] to ensure the solutions were accurate. See Figure 4 for a typical simulation that is compared to the experimental data and model of Stein et al. [27].

The governing equation (2) with diffusion function (3) has six parameters that are unknowns: D_1, D_2, a, n, g, and ν_i. Estimated ranges for some of these parameters can be obtained from Stein et al. [27]. In particular, the migratory diffusion (diffusion when the density u is small), D_1, is estimated to be on the order of 10^{-4} cm^2/day. The growth rate $g \in (0, 1)$/day and the taxis constant

$\nu_i \in (0, 0.02)$ cm/day. However, for a and n, there is no precedent to compare with. We perform a sensitivity study to determine if the model error is insensitive to any of the changing parameters. If we are able to determine that a parameter is insensitive, we will be able to fix its value and not include it as a free variable for parameter optimization.

The error function that we aim to minimize is based on the χ^2 error function used in Stein et al. [27] but modified to account for the experimental data that was made available and uses relative errors for each point. The modified error function that takes into account both how fast the tumor is spreading, by measuring the invasive radius at each day, and also the density of cells by comparing the spatial profile of cells on day 3 is

$$\text{err} = \frac{1}{(N+M)-q-1}\left[\sum_{t=1}^{N}\frac{|r_{\text{data}}(t) - r_{\text{simulation}}(t)|}{r_{\text{data}}(t)} + \sum_{i=1}^{M}\frac{|u_{\text{data}}(3,x_i) - u_{\text{simulation}}(3,x_i)|}{u_{\text{data}}(3,x_i)}\right], \quad (35)$$

where N is the total number of days for which there is invasive radius data, so $N = 7$, M is the total number of cell density data points at day 3, so $M = 17$, and q is the number of parameters being optimized which, in this case, $q = 6$. The first sum in (35) compares the invasive radii of the experimental data, $r_{\text{data}}(t)$, and the simulation, $r_{\text{simulation}}(t)$. The second sum compares the cell density at day 3 at experimental data point x_i for the data, $u_{\text{data}}(3, x_i)$, and the simulation, $u_{\text{simulation}}(3, x_i)$. We use relative errors because the data covers many different orders of magnitude: the cell density is on the order of 10^7–10^8 cells/cm^3 and the invasive radius is on the order of 0.01 cm.

4.1. **Parameter sensitivity.** The parameter sensitivity analysis was performed for the six parameters D_1, D_2, a, n, g, and ν_i such that each was in a physiologically relevant range. The set of base parameters chosen that result in a reasonable match to the data were

$$D_1 = 10^{-4}\,\text{cm}^2/\text{day}, \quad D_2 = 9.99\times10^{-5}\,\text{cm}^2/\text{day}, \quad a = 0.1\,\text{cells/cm}^2,$$
$$n = 1, \quad g = 0.5/\text{day}, \quad \nu_i = 0.01\,\text{cm/day}. \quad (36)$$

These base parameters are not chosen for their excellent fit to the data, rather they are chosen in order to have error that is not too large and to allow for variations to still remain in biologically relevant ranges. To test the sensitivity of one parameter, all the other parameters were held constant and the parameter in question was varied. The results of this sensitivity test is shown in Figure 5.

It is apparent that some parameters are much more sensitive than others, in particular, D_1, g, and ν_i appear to generate the most sensitivity. The results of this sensitivity analysis inform us that all parameters are sensitive and we must take care when we perform our optimization.

4.2. **Parameter estimation.** The parameters are optimized via the MATLAB program fminsearch [12] by minimizing equation (35). Various initial parameter guesses were used as input to ensure parameter values were optimal. The optimized

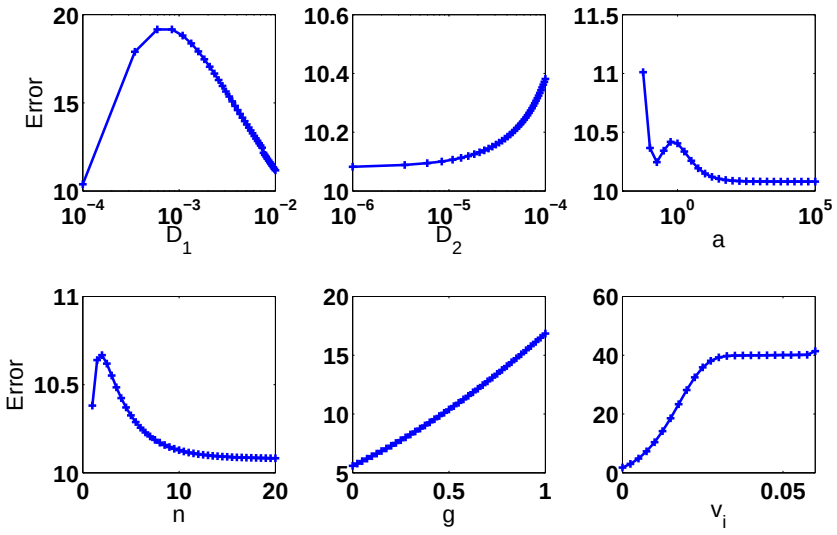

FIGURE 5. Results of a sensitivity analysis with base parameters (36) using error function (35) (vertical axis).

parameters found are

$$D_1 = 5.5408 \times 10^{-6},\ \mathrm{cm}^2/\mathrm{day}, \quad D_2 = 5.3910 \times 10^{-6},\ \mathrm{cm}^2/\mathrm{day},$$
$$a = 0.021188\,\mathrm{cells}/\mathrm{cm}^3, \quad n = 1.2848,$$
$$g = 0.49120/\mathrm{day}, \quad \nu_i = 4.6801 \times 10^{-5}\,\mathrm{cm}/\mathrm{day}. \tag{37}$$

Though $D_1 + D_2$ is very close to 0, it is still the case that $|D_1| > |D_2|$ as necessary. To determine the comparable error to the Stein et al. [27] simulations that use invasive cells as a separate population, we use GRABIT [6] to obtain the simulation data points. Figure 4 shows the results of our simulation with the optimized parameters compared to the Stein et al. [27] simulations and the experimental data.

In the top left panel of Figure 4, the cell density is plotted on the entire domain and it indicates that the model is successful in capturing the behavior of both the tumor core cells and the migratory cells. In the top right panel, the cell density is plotted on a smaller domain and further verifies that our model with one population is relatively as accurate as the model of Stein et al. [27] with the separated invasive cell population and proliferating cell population. In fact, our total error is approximately one-half that of Stein et al. [27] (0.21 compared to 0.45). Even though the simulated invasive radius (in the bottom panel) does not appear to match the experimental data as well, overall there is good agreement between our simulations and the experimental data.

4.3. **Wave speed comparison.** Now that we have shown that our model can be utilized, we compare the analytic minimum wave speed (15) to the wave speed observed in the simulations. To measure the wave speed of tumor spread accurately, we increase the run-time of the simulation to 200 days and enlarge the spatial domain to more so mimic an infinite domain, as is used in the traveling wave

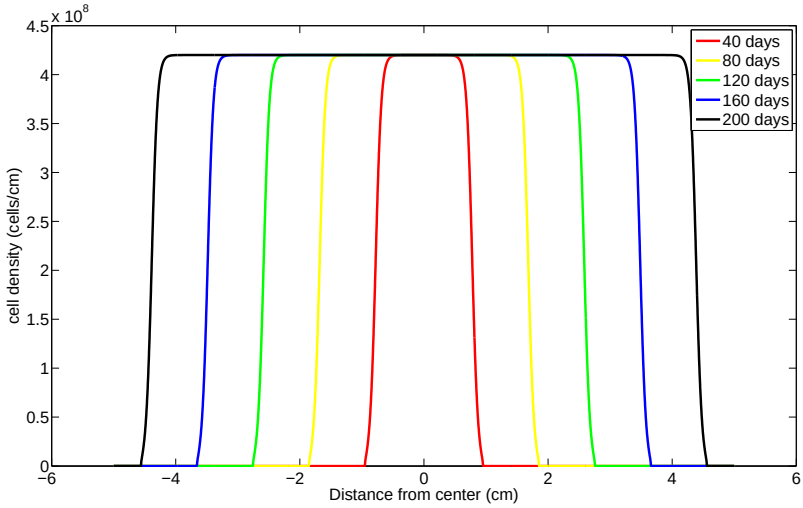

FIGURE 6. Numerical solution of the density-dependent diffusion glioblastoma model (2) with diffusion function (3) and optimized parameter values (37) for days 40, 80, 120, 160, and 200.

analysis. The results of this simulation are shown in Figure 6. The leading edge of the tumor maintains a constant shape and ultimately moves at a constant rate. To estimate the wave speed, we ignore the first few days of the simulation so that the tumor core stably reaches maximum cell density, and then measure the x location where the cell density is last over 2×10^8 cells/cm^3. This is tracked against time, and the MATLAB program polyfit is used to estimate the slope of the curve for a linear fit. Using the optimized parameters (37), the minimum wave speed (15) is $k_{\min} \approx 0.003346$ cm/day and the simulated wave speed $k = 0.02255$ cm/day. While often the observed simulated wave speed is approximately equal to the analytic minimum wave speed, here the simulated wave speed is on the order of 10 times larger than the minimum wave speed.

5. **Discussion and further directions.** We derived a density-dependent diffusion model for in vitro glioblastoma tumor growth that was validated by existing experimental data from Stein et al. [27]. We accurately modeled both the proliferating tumor core as well as the invading migratory cells using only one equation. This model has the potential to simplify glioblastoma tumor modeling—with only one equation the analysis is simpler and simulations can be faster. The existence of traveling waves for this model was studied using phase plane analysis and was corroborated by simulations. We performed a sensitivity analysis and parameter optimization to ensure the model describes the behavior of the tumor.

The governing equation has density-dependent diffusion, logistic growth, and taxis which could possibly be due to chemotaxis or haptotaxis. The chosen density-dependent diffusion function (3) ensures that when the cell density is large, random diffusion is small, and when the cell density is small, random diffusion is large, which could possibly be explained by cell–cell adhesion. This behavior matches how the migratory cells move further away from the tumor core at a large speed, while

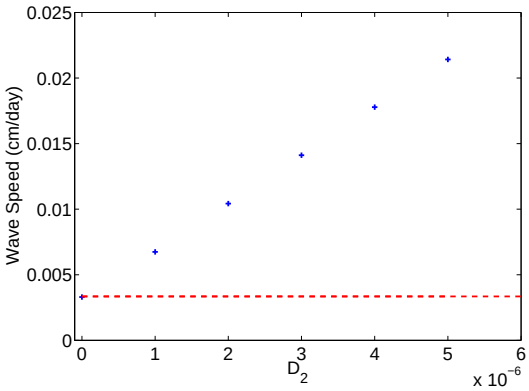

FIGURE 7. The observed simulated wave speed when varying parameter D_2 with all other parameters values (37) fixed. The theoretical minimum wave speed is shown in the red dashed line.

the core remains proliferating and slowly expanding. The logistic term describes the growth of the total number of cells. Taxis describes the active and directed movement of the invasive cells from the tumor core.

A sensitivity analysis indicated that all parameters largely influenced the numerical solutions. We performed a parameter optimization on all six parameters and showed that the error for the best fit was less than the error generated by the two-population model of Stein et al. [27]. This implies that monotone decreasing density-dependent diffusion may better explain the behavior of tumor spheroid cell migration as opposed to cell shedding of the tumor core.

Through wave speed analysis we were able to determine a minimum wave speed and conditions necessary for the existence of traveling wave solutions. Numerical simulations indicated that the observable wave speed is much larger than the analytic minimum wave speed. We conjecture that for monotone decreasing density-dependent diffusion functions, the traveling wave solution with minimum wave speed is unstable.

Furthermore, the observable wave speed appears to depend on other parameters besides D_1, g, and ν_i. Figure 7 indicates that there is a linear relation between parameter D_2 and the observed wave speed, and parameter n also affects the wave speed while a does not affect it as much (results not shown). We also note that when $D_2 = 0$, the observable wave speed equals the analytic minimum wave speed, as expected. A possible explanation for the difference between the analytic and numerical wave speeds could be that nonlinear diffusion can be considered as contributing convection with a "velocity" $-D'(u)\frac{\partial u}{\partial x}$ (in one dimension) but the analytic minimum wave speed was obtained after linearizing the system (11). Further work can be done to investigate finding an expression for the observable wave speed.

Future studies of glioblastoma growth will focus on comparing this model to in vivo data. The model will need to be extended to include brain geometry, and furthermore, comparing the model to in vivo data instead of in vitro data may result in the need to extend the equations to describe more complex behavior such as tumor cell necrosis, brain tissue type differentiation, and mass effect. Instead of density-dependent diffusion, it may be more appropriate to implement anistropy

through diffusion tensor imaging (DTI) such as in the models of Jbabdi et al. [10], Bondiau et al. [3], and Painter and Hillen [21], depending on the availability of experimental data. Another direction is to consider a non-local reaction-diffusion equation instead of density-dependent diffusion with proliferating and dispersing cell groups in which dispersing cells convert proliferating cells into dispersing ones.

Acknowledgments. The authors would like to thank the anonymous reviewers for their careful reading and many helpful suggestions. EMR is partially supported by an Arizona State University research grant and YK is partially supported by an NSF grant DMS 1148771.

REFERENCES

[1] N. J. Armstrong, K. J. Painter and J. A. Sherratt, A continuum approach to modelling cell–cell adhesion, *J. Theor. Biol.*, **243** (2006), 98–113.
[2] C. Atkinson, G. E. H. Reuter and C. J. Ridler-Rowe, Traveling wave solutions for some nonlinear diffusion equations, *SIAM J. Math. Anal.*, **12** (1981), 880–892.
[3] P.-Y. Bondiau, O. Clatz, M. Sermesant, P.-Y. Marcy, H. Delingette, M. Frenay and N. Ayache, Biocomputing: Numerical simulation of glioblastoma growth using diffusion tensor imaging, *Physics in Medicine and Biology*, **53** (2008), p879.
[4] A. Q. Cai, K. A. Landman and B. D. Hughes, Multi-scale modeling of a wound-healing cell migration assay, *J. Theor. Biol.*, **245** (2007), 576–594.
[5] C. Chicone, *Ordinary Differential Equations with Applications*, vol. 34 of Texts in Applied Mathematics, 2nd edition, Springer, 2006.
[6] J. Doke, GRABIT, MATLAB Central File Exchange, `http://www.mathworks.com/matlabcentral/fileexchange/7173-grabit`, (2005), Retrieved July 1, 2014.
[7] B. H. Gilding and R. Kersner, A Fisher/KPP-type equation with density-dependent diffusion and convection: travelling-wave solutions, *J. Phys. A-Math. Gen.*, **38** (2005), 3367–3379.
[8] T. Harko and M. K. Mak, Traveling wave solutions of the reaction-diffusion mathematical model of glioblastoma growth: An Abel equation based approach, *Math. Biosci. Eng.*, **12** (2015), 41–69.
[9] S. Harris, Fisher equation with density-dependent diffusion: Special solutions, *J. Phys. A-Math. Gen.*, **37** (2004), 6267–6268.
[10] S. Jbabdi, E. Mandonnet, H. Duffau, L. Capelle, K. R. Swanson, M. Pélégrini-Issac, R. Guillevin and H. Benali, Simulation of anisotropic growth of low-grade gliomas using diffusion tensor imaging, *Magnetic Resonance in Medicine*, **54** (2005), 616–624.
[11] E. Kengne, M. Saudé, F. B. Hamouda and A. Lakhssassi, Traveling wave solutions of density-dependent nonlinear reaction-diffusion equation via the extended generalized Riccati equation mapping method, *Eur. Phys. J. Plus*, **128** (2013), p136.
[12] J. C. Lagarias, J. A. Reeds, M. H. Wright and P. E. Wright, Convergence properties of the Nelder–Mead simplex method in low dimensions, *SIAM J. Optimiz.*, **9** (1999), 112–147.
[13] P. K. Maini, L. Malaguti, C. Marcelli and S. Matucci, Diffusion-aggregation processes with mono-stable reaction terms, *Discrete Cont. Dyn.-B*, **6** (2006), 1175–1189.
[14] L. Malaguti and C. Marcelli, Travelling Wavefronts in Reaction-Diffusion Equations with Convection Effects and Non-Regular Terms, *Math. Nachr.*, **242** (2002), 148–164.
[15] L. Malaguti, C. Marcelli and S. Matucci, Continuous dependence in front propagation of convective reaction-diffusion equations, *Commun. Pur. Appl. Anal.*, **9** (2010), 1083–1098.
[16] L. Malaguti, C. Marcelli and S. Matucci, Continuous dependence in front propagation for convective reaction-diffusion models with aggregative movements, *Abstr. Appl. Anal.*, **2011** (2011), 1–22.
[17] N. L. Martirosyan, E. M. Rutter, W. L. Ramey, E. J. Kostelich, Y. Kuang and M. C. Preul, Mathematically modeling the biological properties of gliomas: A review, *Math. Biosci. Eng.*, **12** (2015), 879–905.
[18] J. D. Murray, *Mathematical Biology: I: An Introduction*, vol. 17 of Interdisciplinary Applied Mathematics, 3rd edition, Springer, 2002.
[19] W. Ngamsaad and K. Khompurngson, Self-similar solutions to a density-dependent reaction-diffusion model, *Phys. Rev. E*, **85** (2012), 066120.
[20] A. D. Norden and P. Y. Wen, Glioma therapy in adults, *Neurologist*, **12** (2006), 279–292.

[21] K. J. Painter and T. Hillen, Mathematical modelling of glioma growth: The use of Diffusion Tensor Imaging (DTI) data to predict the anisotropic pathways of cancer invasion, *J. Theor. Biol.*, **323** (2013), 25–39.
[22] M. G. Pedersen, Wave speeds of density dependent Nagumo diffusion equations – inspired by oscillating gap-junction conductance in the islets of Langerhans, *J. Math. Biol.*, **50** (2005), 683–698.
[23] V. M. Pérez-García, G. F. Calvo, J. Belmonte-Beitia, D. Diego and L. Pérez-Romasanta, Bright solitary waves in malignant gliomas, *Phys. Rev. E*, **84** (2011), 021921.
[24] F. Sánchez-Garduño and P. K. Maini, Traveling wave phenomena in some degenerate reaction-diffusion equations, *J. Differ. Equations*, **117** (1995), 281–319.
[25] F. Sánchez-Garduño, P. K. Maini and J. Pérez-Velásquez, A non-linear degenerate equation for direct aggregation and traveling wave dynamics, *Discrete Cont. Dyn.-B*, **138** (2010), 455–487.
[26] R. D. Skeel and M. Berzins, A method for the spatial discretization of parabolic equations in one space variable, *SIAM J. Sci. Stat. Comp.*, **11** (1990), 1–32.
[27] A. M. Stein, T. Demuth, D. Mobley, M. Berens and L. M. Sander, A mathematical model of glioblastoma tumor spheroid invasion in a three-dimensional in vitro experiment, *Biophy. J.*, **92** (2007), 356–365.
[28] A. M. Stein, D. A. Vader, L. M. Sander and D. A. Weitz, A stochastic model of glioblastoma invasion, in *Mathematical Modeling of Biological Systems* (eds. A. Deutsch, L. Brusch, H. Byrne, G. Vries and H. Herzel), vol. I of Modeling and Simulation in Science, Engineering and Technology, Birkhäuser Boston, 2007, 217–224.
[29] K. R. Swanson, C. Bridge, J. Murray and E. C. Alvord Jr, Virtual and real brain tumors: Using mathematical modeling to quantify glioma growth and invasion, *J. Neurol. Sci.*, **216** (2003), 1–10.
[30] P. Tracqui, G. Cruywagen, D. Woodward, G. Bartoo, J. Murray and E. Alvord, A mathematical model of glioma growth: The effect of chemotherapy on spatio-temporal growth, *Cell Proliferat.*, **28** (1995), 17–31.
[31] T. P. Witelski, An asymptotic solution for traveling waves of a nonlinear-diffusion Fisher's equation, *J. Math. Biol.*, **33** (1994), 1–16.

Received October 20, 2014; Accepted March 12, 2015.

E-mail address: tstepien@asu.edu
E-mail address: erutter1@asu.edu
E-mail address: kuang@asu.edu